Arctic melt ponds and bifurcations in the climate system

I. Sudakov[a,*], S. A. Vakulenko[b,c], K. M. Golden[a]

[a]*University of Utah, Department of Mathematics, 155 S 1400 E, RM 233, Salt Lake City, UT 84112-0090, USA*
[b]*Institute of Problems in Mechanical Engineering, Russian Academy of Sciences, Bolshoy pr., 61, V.O., St. Petersburg 199178, Russia*
[c]*University ITMO, Kronverkskiy pr., 49, St. Petersburg 197101, Russia*

Abstract

Understanding how sea ice melts is critical to climate projections. In the Arctic, melt ponds that develop on the surface of sea ice floes during the late spring and summer largely determine their albedo – a key parameter in climate modeling. Here we explore the possibility of a conceptual sea ice climate model passing through a bifurcation point – an irreversible critical threshold as the system warms, by incorporating geometric information about melt pond evolution. This study is based on a bifurcation analysis of the energy balance climate model with ice - albedo feedback as the key mechanism driving the system to bifurcation points.

Keywords: sea ice, bifurcations, melt ponds, fractals, stochastic differential equation, phase transitions, climate model.

1. Introduction

Sea ice is not only a sensitive, leading indicator of climate change, it is a key player in Earth's climate system. It also serves as a primary habitat for algal and bacterial communities which sustain life in the polar oceans. Perhaps the most visible, large scale change on Earth's surface in recent decades has been the precipitous decline of summer Arctic sea ice. With this significant loss of a white reflecting surface covering the Arctic Ocean, its albedo or reflectance decreases, and solar radiation is absorbed by the ocean rather than being reflected. This heats the upper ocean, melting even more ice, and so on, which is known as "ice-albedo feedback".

While global climate models predict a general decline in Arctic sea ice over the 21st century, the observed losses have significantly out-paced projections [19, 27]. Improving our predictive capability for the fate of Earth's sea ice cover and its ecosystems depends on a better understanding of important processes and feedback mechanisms. For example, during the melt season the Arctic sea ice cover becomes a complex, evolving

---

[*]Corresponding author

Email addresses: `sudakov@math.utah.edu` (I. Sudakov), `vakulenfr@mail.ru` (S. A. Vakulenko), `golden@math.utah.edu` (K. M. Golden)

mosaic of ice, melt ponds, and open water. The albedo of sea ice floes is determined by melt pond configurations [20, 22, 25]. As ponds develop, *ice-albedo feedback* enhances the melting process. Understanding such mechanisms and their impact on sea ice evolution and its role in the climate system is critical to advancing how sea ice is treated in climate models and improving projections.

Conceptual, or *low order* climate models often introduce feedback through empirical parameterization, for example, taking into account a simple relation between temperature and area of ice covered surface. There is a wide range of such works, including [7, 9, 12, 18]. Usually, ice-albedo feedback was simply associated with a decrease in ice covered area and a corresponding increase in the surface temperature, further decreasing the ice covered area. Given the key role that melt pond formation and evolution plays in sea ice albedo, we note here an apparent lack of incorporation of such features into conceptual models of ice-albedo feedback. Here we note that it is important to explore how melt pond geometry and thermodynamics affect conceptual climate models, and ice-albedo feedback in particular.

While melt ponds form a key component of the Arctic marine environment, comprehensive observations or theories of their formation, coverage, and evolution remain relatively sparse. Available observations of melt ponds show that their areal coverage is highly variable, particularly for first year ice early in the melt season, with rates of change as high as 35 percent per day [22]. Such variability, as well as the influence of many competing factors controlling melt pond and ice floe evolution, make realistic treatments of ice-albedo feedback in climate models quite challenging [22]. Small and medium scale models of melt ponds which include some of these mechanisms have been developed [25, 26], and melt pond parameterizations are being incorporated into global climate models [19].

Moreover, recently it has been found [14] that melt pond geometry has a complex fractal structure, and that the fractal dimension exhibits a transition from 1 to about 2 around a critical length scale of 100 m^2 in area. This behavior should be taken into account in investigating sea ice-albedo feedback.

Given the complex, highly nonlinear character of the underlying differential equations describing climate, it is natural to ask whether the decline of summer Arctic sea ice has passed through a so-called *tipping point*, or irreversible critical threshold as the system progresses toward ice-free summers [1, 9]. A key mechanism potentially driving the system to "tip" is ice-albedo feedback. The main aim of this work is to investigate such a tipping point for a simplified model of sea ice and the climate system which takes into some account the evolution of melt pond geometry and its effect on sea ice albedo.

The surface of an ice floe is viewed here as a two phase composite of dark melt ponds and white snow or ice. The onset of ponding and the rapid increase in coverage beyond the initial threshold is similar to critical phenomena in the theory of phase transitions. Here we ask if the evolution of melt pond geometry − and sea ice albedo − exhibit universal characteristics which do not necessarily depend on the details of the driving mechanisms in numerical melt pond models. Fundamentally, the melting of Arctic sea ice is a phase transition phenomenon, where a solid turns to liquid, albeit on large regional scales and over a period of time which depends on environmental forcing and other factors. We thus look for features which are mathematically analogous to

2

related phenomena in the theories of phase transitions and composite materials.

Basing our approach on the standard nonlinear phase transition model in the 2D case [6], we propose an expression for the rate of change of the melt pond size. It can be extended to the 3D case taking into account the vertical transfer of water to the ocean through ice due to the different physical processes. After that, we introduce the expression for albedo of the ice-covered surface and investigate through the melt pond size how the unexpected fractal geometry of melt ponds [14] can influence the formula for albedo of the ice covered surface.

As the next step, we consider a standard conceptual climate model– an ordinary differential equation (ODE) [12] with ice-albedo feedback taking into account the albedo of melt ponds. We modify this model assuming a stochastic distribution of melt pond sizes, based on the Fokker-Plank equation. After that we investigate equilibria of the resultant stochastic ODE under the key assumption that the surface temperature is a slow function of time relative to melt pond size. Different bifurcation regimes were obtained for this model. One of them may be quite interesting for climate applications, where the temperature of this system is stabilized only due to the fractal transition in melt pond geometry.

2. Evolution of melt ponds

2.1. Mechanism of the fractal transition

Viewed from high above, the sea ice surface can be thought of as a two phase composite of ice and melt water. The boundaries between the two phases evolve with increasing complexity and a rapid onset of large scale connectivity, or percolation of the melt phase (Fig.1). As was shown in [14] that the melt pond perimeter Π can be defined approximately by

$$\Pi \sim \sqrt{S}^D, \tag{1}$$

here S is the area of ponds and D is the the fractal dimension. The authors have observed a transition from $D = 1$ to $D \approx 2$ as the ponds grow in size, with the transitional regime centered around $100 \, \text{m}^2$. According to [14] there exist three regimes:

A) $S < 10 \, \text{m}^2$; then we observe simple ponds with smooth boundaries and $D \approx 1$;

B) $10 \, \text{m}^2 < S < 1000 \, \text{m}^2$; corresponding to transitional ponds where complexity increases rapidly with size;

C) $S > 1000 \, \text{m}^2$; complex, self-similar case, where pond boundaries behave like space filling curves with $D \approx 2$ (so-called fractals).

Here, one can show the transition in empirical formula (1) can be obtained from the rigorous pattern formation theory that uses the Kuramoto-Sivashinsky equation [16]. One can show that beginning with a critical characteristic size, the boundaries become unstable with respect to perturbations along the boundary.

We can suppose pond boundaries with fractal dimension about one can be considered like growing elliptical curves (there are circular ponds, in the ideal case) which become unstable at some characteristic size R, the lengths of the semi-major axe and the semi-minor one are $a_e = r_{e1}R$ and $b_e = r_{e2}R$, respectively, where a_e and b_e have the same order. In the case of fractal transition, the ponds are close to long and narrow
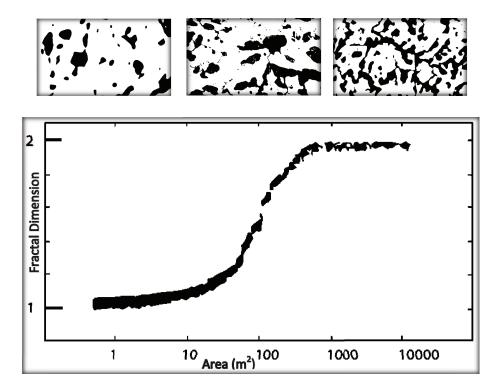
Figure 1: Melt pond fractal dimension *D* as a function of area *S*, showing the transition to complex ponds with increasing length scale. Ponds corresponding to the three regimes are shown to upward: small ponds with smooth boundaries and $D \approx 1$, transitional ponds with a horizontal scale of about 50 m, and complex ponds with river-like boundaries with $D \approx 2$. Adapted from [14].

ellipses, where a_e and b_e have the different order. These ellipses remind one of rivers rather than the simple circular ponds (Fig.1). Then one can expect that the area of such a river of length R is proportional to R.

2.2. Melting front of pond

Our initial considerations of melt ponds will be based on the following geometrical property of melt ponds. Typically, developed ponds have [10, 22] horizontal (characteristic) sizes (R) on the order 10–1000 m, and a small depth (z) of 0.1–0.8 m, i.e. a melting layer has a small but non-zero thickness (see Fig.2). Specific geometric features of melt ponds are determined through fundamental physical processes in sea ice. The complexity of the hydrology and thermodynamics of melt pond formation is the basis for sophisticated numerical models of melt pond evolution [25, 26]. We do not discuss here the details of the thermodynamic processes in sea ice leading to the formation of the melt ponds. However, we can determine melting front (corresponding to the length of the semi-major axis of the elliptical ponds), following by a phase transition model [6] where the melting layer has a small but non-zero thickness and a large
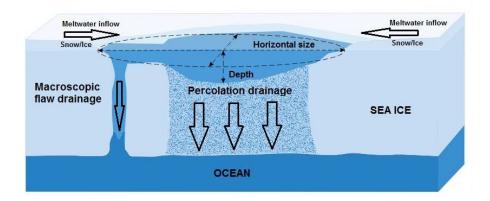
4

Figure 2: Schematic representation of a melt pond. Adapted from [22].

horizontal dimension that agrees with our problem. Also, we can suppose that the ice-water interfaces are quasi one-dimensional, following [17] we obtain the relation for the melting front velocity:

$$v^\star(x, y, z, t) = \delta(T) \tag{2}$$

where $v^\star$ is the normal melting front velocity at the point (x, y, z) and δ is a function of melting surface temperature T. The quantity δ can be expressed via microscopic parameters of the phase transition problem [6, 11, 17], however, it is simpler to find this quantity by experimental data since δ determines the main contribution in the pond area increasing.

We are planning to consider the planar case. In this case, our fronts are curves. All fronts are closed curves, which initially are not too different from ellipses. For elliptical fronts of size $R(t)$, Eq. (2) takes the form

$$\frac{dR}{dt} = \delta(T), \tag{3}$$

Some actual melt ponds can be thought of as three dimensional lenses (see Fig.2). In [22] some important effects are described and experimental data are presented. It is shown that there is a vertical transfer of water in the ocean through ice percolation, permeability, or macroscopic flows, which is proportional to the depth of the lens. We can assume that on average this depth is proportional to the pond size R. Therefore, due to this effect, a rough estimate of the rate dW/dt of the water mass in the pond is $-\beta W$. Since $W = const R^3$, we have the following contribution R_w of this effect into dR/dt: $R_w = -\gamma R$. Taking into account this effect, we change Eq.(3) into the form

$$\frac{dR}{dt} = \delta(T) - \gamma(T)R = P(R, T), \tag{4}$$

where we suppose that δ and γ depend on the temperature.

5

2.3. Melt ponds and albedo

Albedo is the reflecting power of a surface. Material properties, surface topography, and other properties of the surface influence albedo as well as related feedback mechanisms. We will involve melt ponds in the feedback by means of area. For this aim we apply formula (1) to study the melt ponds area.

The total average albedo A can be approximated by

$$A = A_{rp}\frac{S_{rp}}{S_{rp}+S_{arc}} + A_{arc}\frac{S_{arc}}{S_{rp}+S_{arc}}, \tag{5}$$

where S_{arc} is the area of the Arctic zone covered by ice for low temperatures and S_{rp} is the area of the rest planet, A_{rp} is the average albedo of the rest planet, and A_{arc} is the average albedo of Arctic zone.

According [10], the albedo of the Arctic surface is

$$A_{arc} = A_0(1 - S_r) + B_0 S_r = A_0 - (A_0 - B_0)S_r, \tag{6}$$

where A_0 is an average albedo of ice area, B_0 is an average albedo of melt ponds, the percentage of the surface covered by ponds: $S_r = \frac{S_{melt}}{S_{arc}}$ with S_{melt} – the average area of all melt ponds. Thus, we have obtained the formula for albedo involving the area of the surface covered by melt ponds.

Using the facts about the fractal transition we compute the melt pond area as follows. For the averaged size $R(t) < R_F$, again we assume that shape of melts ponds are close to ellipses. Then we define the area of melt ponds by

$$S_{melt}(\mathbf{R}) \approx \pi c_1 \sum_{i=1}^{N} R_i(t)^2, \quad S_{melt} < s_* N \approx N\pi c_1 R_F^2 \tag{7}$$

the coefficient c_1 takes into account a deviation of elliptical form, R_F is a critical characteristic size of melt pond at the fractal transition. Here $\mathbf{R} = (R_1(t),...,...R_N(t))$ is a vector of pond sizes and N is the number of the ponds. For $R > R_F$ the ponds can be envisioned as long and narrow (albeit contorted). The ellipse area is $\pi a_e b_e$, where a_e, b_e are semi-major and semi-minor axis. We suppose that after the fractal transition a_e weakly depends on the size parameter R_i whereas b_e is proportional to R_i. Then we use the relation

$$S_{melt}(\mathbf{R}) \approx c_2 \sum_{i=1}^{N} R_i(t), \quad S_{melt} > s_* N, \tag{8}$$

where c_2 is a constant, which determines a characteristic average width of river-like ponds (that we observe after the fractal transition).

3. Low order climate model with ice-albedo feedback for melt ponds

In the previous sections, we have obtained expressions for the albedo involving the percentage of the surface covered by melt ponds, which depends on the area of the ponds. In turn, the area evolution depends on melt pond dynamics. This can be

explored in a conceptual climate model. Such models are based on an ice-albedo feed-back that allows albedo to be temperature dependent. These models couple the albedo to the global energy balance through inclusion of heat transport [7, 18]. In this section we show how these models can be developed taking into account melt pond character-istic size dynamics. It is based on a relationship between albedo, melt pond size, and temperature. It allows us to find a climate bifurcation point related to melt ponds, and estimate climate sensitivity provided that melt ponds play a key role in the mechanism of ice-climate feedback.

A simple climate model is a one-dimensional system which can be described [12] by

$$\frac{dT}{dt} = \frac{1}{\lambda}(-\varepsilon\sigma T^4 + \frac{\mu_0 I_0}{4}(1-A)),\tag{9}$$

where λ is thermal inertia, T is surface temperature, t is time, and A is the albedo of the surface. The left term characterizes the time-dependent behavior of the climate system, usually taken to mean an average surface temperature. Surface temperature changes as a result of an imbalance in radiative heat transfer. On the right hand side, the first term is outgoing emission and the second term represents incoming solar radiation. Gener-ally, incoming solar radiation to earth's surface should depend on total solar radiation incident on earth (μ_0), and the solar constant (I_0) as well as surface albedo. On the other side, outgoing emission can be described through the fourth power of temperature, the effective emissivity (ε) and a Stefan-Boltzmann constant (σ).

Substituting the formula (5) via the pond characteristic size, we finally have the following system for R_i, T:

$$\frac{dT}{dt} = f(\mathbf{R}, T),\tag{10}$$

where the right hand side is a sum of two terms that describe, the contributions of land albedo, land emissivity and arctic albedo, respectively:

$$f(\mathbf{R}, T) = F_{rp}(T) + F_{arc}(S_{melt}(\mathbf{R})),$$

where

$$F_{rp}(T) = \frac{1}{\lambda}(-\varepsilon\sigma T^4 + \frac{\mu_0}{4}I_0(1-A_{rp}(T))),\tag{11}$$

$$F_{arc}(\mathbf{R}, T) = \frac{\mu_0 I_0}{4\lambda}(A_0 - (A_0 - B_0)S_{melt}(\mathbf{R})/S_{arc}).\tag{12}$$

Here we assume, for simplicity, that $A_{rp}(T)$ is a regular function of averaged tempera-ture T, which weakly depends on T at some value T_s. This value defines the averaged surface temperature for the case when all Arctic is covered by ice, i.e., $S_{melt} = 0$:

$$F_{rp}(T) + F_{arc}(0) = 0\tag{13}$$

(following here ideas from [4] and [5]).

For R_i we use the equation

$$dR_i = P(R_i, T)dt + 2\kappa d\omega_i,\tag{14}$$

where $i = 1, ..., N$ and κ is a parameter. Here, observing that pond growth can be viewed as a stochastic process as was presented in [29], we use the Langevin equation for R_i, where $d\omega_i$ are independent standard Wiener processes. Since $N >> 1$ we can also use the Fokker-Planck equation for the pond size distribution $\rho(R_i, t)$:

$$\frac{\partial \rho}{\partial t} = -\frac{\partial P(R_i, T)\rho}{\partial R_i} + \kappa^2 \frac{\partial^2 \rho}{\partial R_i^2}.$$

(15)

This model involves the additive noise generated by the term $\kappa d\omega_i$. Such models are standard, have many applications and well studied, see [15]. We need such a term in order to obtain a reasonable pattern of pond sizes for large t since otherwise we obtain that all the ponds have the same size as $t >> 1$. Moreover, the stochastic model allows us to describe stochastic resonance effects [4,5], which are possible here.

This nonlinear climate model can be reformulated as a stochastic dynamical system. Note that for $R_i > R_0$, $\kappa = 0$ (when stochastic effects are absent), and with increasing $\delta(T)$ one has

$$\frac{\partial f(R_i, T)}{\partial R_i} > 0, \quad \frac{\partial P(R_i, T)}{\partial T} > 0.$$

This means that the system (10) is cooperative. Therefore, due to fundamental results of M. Hirsch [13], this system cannot exhibit oscillating solutions and the Andronov–Hopf bifurcations [3]. All trajectories converge to equilibria and the attractor is a union of these equilibria.

This observation allows us to compute the pond area S_{melt} for large times. In physically realistic situations $N >> 1$, so we can simplify the approximations Eqs. (7) and (8). We can transform these relations as follows

$$S_{melt} \approx S_c = \pi c_1 N \int_0^\infty R_i^2 \rho(R_i, t) dR_i,$$

(16)

for $S_c < s_* N$, where $s_* = \pi c_1 R_F^2$, and c_1 is a constant taking into account the deviation from the elliptical pond form.

After the fractal transition one has

$$S_{melt} \approx S_F = c_2 N \int_0^\infty R_i \rho(R_i, t) dR_i,$$

(17)

for $S_c > s_* N$. Here $\rho(R_i, t)$ can be defined by Eq. (15).

4. Analysis of the system for temperature and ponds

Equilibria of the system (10) and (14) for $\kappa = 0$ can be found as follows. For fixed temperature T we compute quasi-equilibria $R_i(T)$ setting $P(R_i, T) = 0$. This equation has the root

$$R_+(T) = \frac{\delta(T)}{\gamma(T)}.$$

(18)

Note that the root R_+ is a stable resting point (a local attractor) of a semi-flow defined by Eq. (10). Therefore, the dynamics of Eq. (10) can be described as follows: $R_i(t) \rightarrow R_+$ for large times.

Our key assumption is that T is a slow function of time relative to $R_i(t)$, i.e., the melting process for ponds is fast while changing of the related climate system is slow.

Under this assumption computing equilibria for the temperature T becomes a mathematically tractable problem even in the stochastic case $\kappa > 0$. In fact, then (using classical results of dynamical systems theory) we solve the Fokker-Planck equation (15) for each fixed T, after which we substitute the results in Eq. (9) and find the equilibria for T. So, let us fix T in Eq. (15). It is well know that $\rho(R_i, t) \rightarrow \rho_{eq}$ for large times t, where ρ_{eq} is an equilibrium distribution defined by

$$\rho_{eq} = C(T) \exp(-\kappa^{-2} V(R, T)), \tag{19}$$

with

$$V(R, T) = \delta(T)R - 0.5\gamma(T)R^2,$$

where $C(T)$ is a factor such that $\int_0^\infty \rho_{eq}(R)dR = 1$. We have then

$$S_{melt} = \pi c_1 N C(T) \int_0^\infty R^2 \exp(-\kappa^{-2} V(R, T))dR, \tag{20}$$

before the fractal transition and

$$S_{melt} = c_2 N C(T) \int_0^\infty R \exp(-\kappa^{-2} V(R, T))dR, \tag{21}$$

after this transition. Therefore, for small κ we obtain the following relations for the pond area S_{melt} (using that the function ρ_{eq} is well localized at $R = R_+(T)$)

$$S_{melt}(T) = C_0 N (R_+(T))^2, \tag{22}$$

for $R_+(T) < R_F$, and

$$S_{melt}(T) = C_0 N R_+(T) R_F \tag{23}$$

for $R_+(T) \geq R_F$. Here C_0 is a constant and R_F is a critical characteristic size of melt pond at the fractal transition. We assume that $R_+(T)$ is an increasing function of T, i.e., $\frac{dR_+(T)}{dt} > 0$. This assumption looks natural. Note that $S_{melt}(T)$ has such properties. This function is continuous and has a derivative $dS_{melt}/dT = S'_{melt}(T)$, which has a break at the temperature T_F such that $S_{melt}(T_F) = R_F$.

For the temperature T, as a result of some straight forward transformations, we obtain then the evolution equation

$$\frac{dT}{dt} = G(T), \tag{24}$$

where

$$G(T) = \zeta(T) - Q(T), \tag{25}$$

There are

$$\zeta(T) = \frac{4\varepsilon\sigma T^4 (S_{rp} + S_{arc})}{\mu_0 I_0 S_{arc}} + A_{rp}(T)\frac{S_{rp}}{S_{arc}} + A_0$$

9

and

$$Q(T) = (A_0 - B_0)\frac{S_{melt}(T)}{S_{arc}}.$$

The equilibria of this equation are defined by

$$Q(T) = \zeta(T). \tag{26}$$

These equilibria are intersections T_{eq} of the curves $\zeta(T)$ with $Q(T)$. If for T_{eq} one has

$$\zeta'(T_{eq}) < Q'(T_{eq}),$$

then the intersection gives us a stable equilibrium and and thus a local attractor, otherwise this equilibrium is a saddle point.

Note that the function $Q(T)$ equals zero for $T < T_b$, where T_b is the temperature of the phase transition, when we have no melt ponds, it grows faster in T for smaller T while the averaged pond size is less than the critical value around R_F. This means that early in the warming cycle we observe fast growth and afterwards when the ponds become fractals, the growth of $Q(T)$ in T is slower. This result is consistent with experimental data [22].

The analysis of Eq.(26) can proceed if we take into account that $S_{arc} << S_{rp}$ and, moreover, supposing that melting phenomena appear at some temperature interval T_0, T_1, following [4,5] note that T^4 and $A_{rp}(T)$ vary insignificantly on this range. The the problem can be further simplified by a linearization of $\zeta(T)$ at the temperature T_s which is an equilibrium averaged surface temperature of the system "The rest of the planet + the Arctic zone", where $S_{melt} = 0$. We have

$$\zeta(T_s) = 0$$

and, following [2], consider $Q(T)$ as a small but sufficiently irregular in T perturbation. By an elementary perturbation theory, we have that the temperature T is defined by

$$\zeta'(T_s)(T - T_s) = Q(T). \tag{27}$$

Depending on the parameters $A_0 - B_0$, S_{arc}/S_{rp}, $\beta = \frac{\mu_0 I_0}{4\varepsilon\sigma}$, and others there are possible such main cases:

(**I**) a single stable equilibrium which serves as a global attractor, Fig. 3;

(**II**) a stable and unstable equilibria, Fig. 4;

(**III**) two stable equilibria plus a saddle point, Fig. 5.

A bifurcation picture occurs if we assume that $Q(T)$ is close to 0 for $T < T_b$, and increasing for $T > T_b$. This condition looks natural since for low temperatures melt ponds are frozen.

We can take the following approximation, when Eq. (27) can be solved analytically. Let us set $S_{melt} = 0$ for $T < T_b$. For $T > T_b$ we use relations (22) and (23) with some $C_0 \approx \pi$ and $R_+(T) \approx r_0(T - T_b)$, where $r_0 > 0$ is a parameter, which determines the pond size increase in temperature T. Such an approximation means that we use linear approximations for $\delta(T)$ and $\gamma = const$ for $T > T_b$. Then Eq. (27) becomes

$$B_p(T - T_s) = (A_0 - B_0)\frac{S_{melt}(T)}{S_{arc}} = Q(T),$$

$$B_p = \frac{4\varepsilon\sigma T_s^3}{I_0\mu_0/4} - a_p, \quad a_p = \frac{dA_{rp}(T)}{dT}\Big|_{T=T_s}, \tag{28}$$
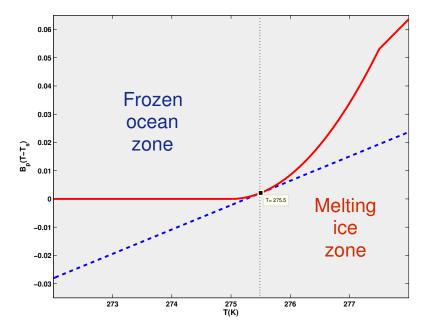
Figure 3: This picture illustrates the bifurcation, here $T_{eq} = 275.50$ K is a single equilibrium value. The dotted blue line corresponds to the term $B_p(T - T_s)$ in the equation (28) and the red curve is $Q(T) = (A_0 - B_0)\frac{S_{melt}(T)}{S_{arc}}$. The steady state value of T can be obtained as intersections of these curves.

where the right hand side is zero for $T < T_b$, it is quadratic function in T for $T \in (T_b, T_F)$ and it is a linear function for $T > T_F$.

Note that Eq. (28) can have $n = 1, 2$ or $n = 3$ roots and it is also possible that the roots are absent. We consider B_p as a bifurcation parameter for the next two cases: **A** the fractal transition is absent; **B** in presence of this transition.

A. Here the plot of $Q(T)$ is a parabolic curve. Therefore, for small B_p there are no roots of Eq. (28), for some $B_p = B_*$ we have a single root, and for $B_p > B_*$ one has two roots, and only a single one is stable, whereas the second one is unstable. Remind that the saddle-node (SN) bifurcation corresponds to situation, in which, as a bifurcation parameter goes a critical value, two fixed points (or equilibria) of a dynamical system collide and annihilate each other. The pitchfork bifurcation occurs when we have a stable equilibria, after two equilibria (at a bifurcation point) and finally three equilibria (one equilibrium is a saddle point and unstable, other two ones are stable). Therefore, in the case **A** we are dealing with the SN bifurcation (since n take the values $0, 1$ and 2).

B. In this case situation is much more complicated. First, the bifurcation obtained for the case **A** also appears but now it can be classified as a pitchfork bifurcation.
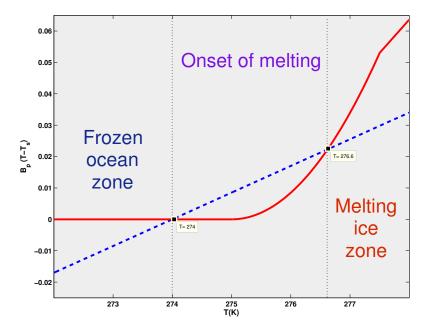
11

Figure 4: Here we see the case of two equilibria. We have a stable equilibria at $T_{eq} = 274.00$ K and a unstable one at $T_{eq} = 276.60$ K (for stable equilibria T_{eq} one has $B_p > Q'(T_{eq})$). The dotted blue line corresponds to the term $B_p(T - T_s)$ in the equation (28) and the red curve is $Q(T) = (A_0 - B_0)\frac{S_{melt}(T)}{S_{arc}}$. The steady state value of T can be obtained as intersections of these curves.

Moreover, we observe the new effects. The main new effect is a second bifurcation and formation of new equilibria. To see it, let us note, that the graph of $Q(T)$ is a parabolic curve on some interval. After the fractal transition this graph is a right line: $Q(T) = Q(T_F) + q_c(T - T_F)$, where $q_c > 0$ is a coefficient (see Figs. 3, 4, 5). Consider the number n of the roots of Eq.(28) as a function of B_p. Assume this parameter increases from 0 to $+\infty$. If q_c is not too large, then for very small B_p there no roots $n = 0$, after $n = 1$ and for $B_p = B_*$ we have $n = 2$ (here the first SN bifurcation occurs), and for $B_p > B_*$ we have $n = 3$. The bifurcation point is not influenced by the fractal transition but this transition gives us an additional stable equilibrium formed by the intersection between $B_p(T - T_s)$ and the right line $Q(T_F) + q_c(T - T_F)$. For $n = 1$ we have a single stable equilibrium, for $n = 3$ we obtain two stable equilibria and a saddle point. As it was explained above, this situation corresponds to a pitchfork bifurcation. Thus, the fractal transition changes a bifurcation type.

Furthermore, a new bifurcation occurs when $n = 2$ when the intersection point of the curves $B_p(T - T_s)$ and $Q(T)$ corresponds to the value $T = T_F$. We obtain then $n = 2$ and for larger B_p we have $n = 1$. This second bifurcation also is a pitchfork one, which
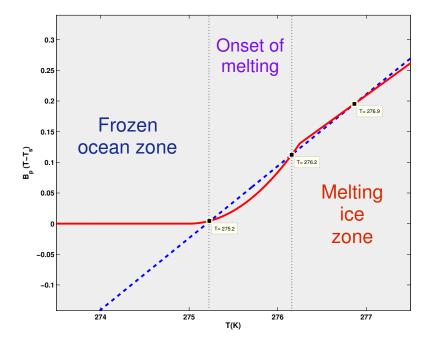
12

Figure 5: This plot shows the case of three equilibria. A stable equilibria T_{eq} are 275.24, 276.20 and 276.90 K. The blue dotted line corresponds to the term $B_p(T - T_s)$ in the equation (28) and the red curve is $Q(T) = (A_0 - B_0)\frac{S_{melt}(T)}{S_{arc}}$. The steady state value of T can be obtained as intersections of these curves.

goes in an inverse direction. Finally, we observe that, as B_p increases, n takes the value $0, 1, 2, 3, 2, 1$ and that the fractal transition leads to two pitchfork bifurcations.

A similar geometric arguments show that for large q_c the number n takes the values $0, 1, 2, 1$. Here we obtain two saddle-node bifurcations (the first one is illustrated by Fig. 3).

Note that for $\tau = T_s - T_b > 0$ three equilibria are possible if and only if the following conditions hold:

$$v \in (1/2, 1), \quad u > v(1 - v), \quad u < 1/4,$$

where

$$b = (A_0 - B_0)C_0Nr_0^2/(B_pS_{arc}), \quad u = b\tau, \quad v = b(R_F/r_0).$$

Here, we list the parameters, which were used for Figs. 3, 4, 5. There are effective emissivity $\varepsilon = 0.62$, average albedo of ice area $A_0 = 0.68$, Stefan-Boltzmann constant $\sigma = 5.67 \cdot 10^{-8}\,\mathrm{J \cdot s^{-1}m^{-2}K^{-4}}$ average albedo of melt ponds $B_0 \approx 0$, $\mu_0 = 1.00$ and incoming solar energy $I_0/4$ is 340.00 W·m^{-2}. We have put $S_{arc} = 5.00 \cdot 10^{12}\,\mathrm{m}^2$ and $a_p = 0$. The number N of the ponds is $N \approx 4.00 \cdot 10^8$. In case of Fig.3 there are $R_F = 35.00$ m, $r_0 = 3.00$ m/K, $T_b = 275.00$ K, $T_s = 274.50$ K. For Fig. 4 the parameters

13

are $r_0 = 7.00$ m/K, $T_s = 276.00$ K, $T_b = 275.00$ K and $R_F = 17.50$ m. The parameters $R_F = 25.00$ m, $r_0 = 20.00$ m/K, $T_b = 275.00$ K, $T_s = 275.20$ K are used in Fig. 5.

5. Discussion

In this section, we discuss some physical consequences of the obtained results.

5.1. Melt pond evolution and sea ice melt pond area.

First of all, we discuss the different regimes of our toy climate system related to bifurcations that can happen in this system. In the case of saddle-node bifurcation we have two stable zones: "Frozen ocean" and "Melting ice", see Fig.3. Such kinds of climate states were described in the earliest works [7, 18]. We can explain its existence through the phase transition. However, the other two cases are more interesting.

In the case of two equilibria (Fig.4), we can distinguish three different zones. Two of them are similar to the first case "Frozen ocean" and "Melting ice", however we introduce a new zone between two equilibria: "Onset of melting". This zone corresponds to the initial growth of melt ponds with the elliptical shapes. Physically, the existence of this zone plays an important role, because seasonal sea ice minimum strongly correlates with beginning melt pond fraction as was shown in [24], based on statistical analysis of data from models. In this paper, it is shown that this zone, which is located between two stable and unstable equilibria, determines the future state of this system. However, here we can suppose that in the "Melting ice" zone growing ponds will cover a significant ice surface that will lead to full ice disappear in during one season.

In the case of three equilibria (Fig.5), we still distinguish three different zones: "Frozen ocean" subsists due to the low temperature; "Onset of melting" still exists, however in this case it is shorter, because the elliptical ponds shifts its shapes very fast to narrow and long rivers due to the fractal transition, which corresponds to the second point of equilibrium. Crossing this point, the melt ponds are approaching to the complex fractal forms. Such fractal system stabilizes our simple climate system at the third point of equilibrium. After that point the pond growth is absent. Computations show that in the second case the area S_{melt} covered by ponds is $1.60 \cdot 10^{11}$ m^2 at $T_{eq} = 276.60$ K, but in the third case the area S_{melt} covered by ponds is significantly less $0.27 \cdot 10^{11}$ m^2 at $T_{eq} = 276.90$ K. Thus, we can conclude melt ponds help to prevent full summer Arctic sea loss, because they can stabilize the state of the climate system due to the fractal transition. In addition, existence of "Onset of melting" zone due to the transition from stable to unstable equilibria allows to control the amount of sea ice extent by the end of the melting ice season.

In addition, we can consider another parameter which can control the physical state of the system: there is a thermal inertia λ (Eq.(9)). A huge heat capacity of the ocean produces the thermal inertia that can make surface of melting or freezing more gradual. In our model the parameter λ defines a rate of the system approaching to an equilibrium. Usually, conceptual models take into account this parameter as a constant, however in case of melt pond incorporated models this parameter may be defined as a function, then the rate of reaching equilibrium will be easily computed. It can help to understand how fast a bifurcation may happen. However, these models should

14

incorporate more complicated thermodynamics of the ocean-atmosphere interaction, at least, a model such as was suggested in [9].

5.2. *Melt ponds evolution and critical behavior of albedo.*

From the first appearance of visible pools of water, often in early June, the area fraction of sea ice covered by melt ponds can increase rapidly to over 70 percent in just a few days. Moreover, the accumulation of water at the surface dramatically lowers the albedo where the ponds form. A corresponding critical drop-off in average albedo [22]. The resulting increase in solar absorption in the ice and upper ocean accelerates melting [21], possibly triggering ice-albedo feedback. Similarly, an increase in open water fraction lowers albedo, thus increasing solar absorption and subsequent melting. The spatial coverage and distribution of melt ponds on the surface of ice floes and the open water between the floes thus exerts primary control of ice albedo and partitioning of solar energy in the ice-ocean system [8, 22].

Thus, each data set exhibits critical behavior at the onset of melt pond formation, similar to the behavior of order parameters characterizing phase transitions in thermo-dynamics.

We would like to discuss such critical behavior related to melt pond evolution based on our model. Here, we are taking into account that the melt pond size is a fast variable, and the surface temperature (time-averaged) is a slow variable. Therefore, the mean size depends on the temperature. Also, $\delta(T)$ and $\gamma(T)$ in Eq. (4) are close to constant (or slightly changing as a function of T). In this case, the size is a smooth function of the temperature. When the critical size is changing due to the fractal transition, functions of melt pond area have a jump at this point(see Eqs. (7), (8)). According to formula (6) the albedo depends linearly on area. So, we can approximate albedo as a hyperbolic tangent (see Fig. 6) of the average surface temperature($\bar{T}$):

$$A(\bar{T}) \approx A_F + A_m \tanh(T_\Delta) \tag{29}$$

where A_F is the albedo of the surface after the fractal transition, and A_m – the constant corresponds to the change in albedo due to the fractal transition, T_Δ – changing in the surface temperature due to the fractal transition [22]. Previously, this formula was introduced empirically, based on the observation data. However, we may see physical interpretation of this phenomenon: the transition in fractal dimension of melt ponds affects the shape of the albedo curve.

6. Conclusions

In this work, we have addressed some fundamental questions related to the role of sea ice in the climate system. First of all, we considered how geometrical properties of melt ponds can influence ice-albedo feedback and how it can influence the bifurcation structure of a simple climate model. The melting pond growth model is developed to study melt pond formation and its changes in geometry. The approach, proposed here, can be useful for future investigations of the geometry of melt ponds and their evolution.
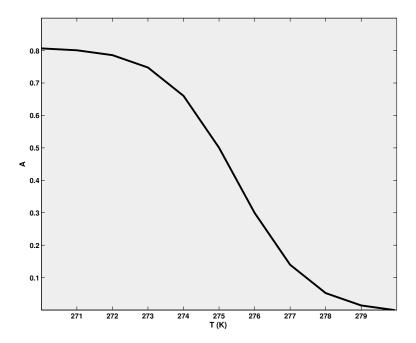
Figure 6: Albedo as a hyperbolic function of the average surface temperature due to the fractal transition in the melt pond geometry.

We reviewed a low-order energy balance climate model using standard methods of dynamical systems theory. As a result, we see different behavior of the climate system in the case of the ice-albedo feedback with melt pond following a stochastic distribution for the sizes. We concluded that in this case melt ponds can strengthen the positive feedback and lead the climate system through a bifurcation point. Moreover, the melt pond contributions can have a significant influence on the temperature state of the climate system.

We would like to emphasize that in this research three scales of the problem were connected. We have tied up micro, macro and global scales through the relation for albedo. Albedo (global scale) contains the area of melt ponds (expressed through sizes – macro scale) which in turn is connected to the microscopic parameters describing thermodynamic changes in the melting front. Thus, this research advances the multiscale approach to tipping point investigations, first presented for permafrost lakes in [28].

Acknowledgments

References

[1]   Abbot, D. S., Silber, M. & Pierrehumbert, R. (2011) Bifurcations leading to summer arctic sea ice loss. *J. Geophys. Res. Atmos.*, **116**, D19120, doi:10.1029/2011JD015653.

[2]   Abbot, D. S., Voigt, A. & Koll D. (2011) The Jormungand global climate state and implications for Neoproterozoic glaciations. *J. Geophys. Res. Atmos.*, **116**, D18103, doi:10.1029/2011JD015927.

[3]   Arnold, V. I. (1983) *Geometrical methods in the theory of ordinary differential equations*. Grundlehren Math. Wiss., Springer.

[4]   Benzi, R., Parisi, G., Sutera, A. & Vulpiani, A. (1983) A theory of stochastic resonance in climatic change. *SIAM J. Appl. Math.*, **43**, 565–578.

[5]   Berglund, N. & Gentz, B. (2002) Metastability in simple climate models: pathwise analysis of slowly driven Langevin equations. *Stoch. Dynam.*, **2**, 327–356.

[6]   Caginalp, G. (1989) Stefan and Hele-Shaw type problems as asymptotic limits of the phase field equations. *Phys. Rev. A*, **39**, 5887–5896.

[7]   Curry, J. A., Schramm, J. & Ebert, E. E. (1995) On the sea ice albedo climate feedback mechanism. *J. Climate*, **8**, 240–247.

[8]   Eicken, H., Grenfell, T. C., Perovich, D. K., Richter-Menge, J. A. & Frey, K. (2004) Hydraulic controls of summer Arctic pack ice albedo. *J. Geophys. Res. Oceans*, **109**, C08007.

[9]   Eisenman, I. & Wettlaufer, J. S. (2009) Nonlinear threshold behavior during the loss of Arctic sea ice. *Proc. Natl. Acad. Sci. U.S.A.*, **106**, 28-32. doi:10.1073/pnas.0806887106.

[10] Fetterer, F. & Untersteiner, N. (1998) Observations of melt ponds on Arctic sea ice. *J. Geophys. Res. Oceans*, **103**, 24821-24835.

[11] Fife, P. C. & Penrose, O. (1995) Interfacial dynamics for thermodynamically consistent phase-field models with nonconserved order parameter. *Electron. J. Differential Equations*, **16**, 1–49.

[12] Fraedrich, K. (1979) Catastrophes and Resilience of a zero-dimensional climate system with ice-albedo and greenhouse feedback. *Q. J. R. Meteorol. Soc.*, **105**, 147–167.

[13] Hirsch, M. W. (1984) The dynamical systems approach to differential equations. *Bull. A. M. S.*, **11**, 1–64.

[14] Hohenegger, C., Alali, B., Steffen, K. R., Perovich, D. K. & Golden, K. M. (2012) Transition in the fractal geometry of Arctic melt ponds. *Cryosphere*, **6**, 1157–1162, doi:10.5194/tc-6-1157-2012.

[15] Horsthemke, W. & Lefever, R. (2006) *Noise-Induced Transitions: Theory and Applications in Physics, Chemistry, and Biology*. Springer Series in Synergetics, Vol. 15, Springer Science and Business Media.

[16] Langer, J. S. (1987) *Lectures in the theory of pattern formation*, in: *Chance and Matter*, Souletie, J., Vannimeus, J. & Stora, R., eds., North-Holland, Elsevier Science Publishers.

[17] Molotkov, I. & Vakulenko, S. (1988) *Nonlinear localized waves*. Leningrad University Publishing.

[18] North, G. R. (1975) Theory of energy-balance climate models. *J. Atmos. Sci.*, **32**, 2033–2043.

[19] Pedersen, C. A., Roeckner, E. Luthje, M. & Winther, J. (2009) A new sea ice albedo scheme including melt ponds for ECHAM5 general circulation model. *J. Geophys. Res. Atmos.*, **114**, D08101, doi:10.1029/2008JD010440.

[20] Perovich, D. K., Light, B., Eicken, H., Jones, K. F., Runciman, K. & Nghiem, S. V. (2007) Increasing solar heating of the Arctic Ocean and adjacent seas, 1979-2005: and role in the ice-albedo feedback. *Geophys. Res. Lett.*, **34**, L19505, doi:10.1029/2007GL031480.

[21] Perovich, D. K., Richter-Menge, J. A., Jones, K. F. & Light, B. (2008) Sunlight, water, and ice: Extreme Arctic sea ice melt during the summer of 2007. *Geophys. Res. Lett.*, **35**, L11501, doi:10.1029/2008GL034007.

[22] Polashenski, C., Perovich, D., & Courville, Z.(2012) The mechanisms of sea ice melt pond formation and evolution. *J. Geophys. Res. Oceans*, **117**, C01001, doi:10.1029/2011JC007231.

[23] Sankelo, P., Haapala, J., Heiler, I. & Rinne, E. (2010) Melt pond formation and temporal evolution at the drifting station Tara during summer 2007. *Polar Research*, **29(3)**, 311–321.

[24] Schroder D., Feltham, D. L., Flocco, D. & Tsamados, M. (2014) September Arctic sea-ice minimum predicted by spring melt-pond fraction. *Nat. Clim. Chang.* **4**, 353–357, doi: 10.1038/NCLIMATE2203.

[25] Scott, F. & Feltham, D. L.(2010) A model of the three-dimensional evolution of Arctic melt ponds on first-year and multiyear sea ice. *J. Geophys. Res. Oceans*, **115 (C12)**, C12064, doi: 10.1029/2010JC006156.

[26] Skyllingstad, E. D. & Paulson, C. A. (2007) A numerical simulations of melt ponds. *J. Geophys. Res. Oceans*, **112**, C08015, doi:10.1029/2006JC003729.

[27] Stroeve, J., Holland, M. M., Meier, W., Scambos, T. & Serreze, M. (2007) Arctic sea ice decline: Faster than forecast. *Geophys. Res. Lett.*, **34**, L09591, doi: 10.1029/2007GL029703.

[28] Sudakov, I. & Vakulenko, S. (2014) A mathematical model for positive permafrost carbon-climate feedback. *IMA J. Appl. Math.*, doi:10.1093/imamat/hxu010.

[29] Yackel, J. J., Barber, D. G. & Hanesiak, J. M. (2000) Melt ponds on sea ice in the Canadian Archipelago 1. Variability in morphological and radiative properties. *J. Geophys. Res. Oceans*, **105**, 3054–3075, doi:10.1002/2013JC009617.